Influence of Geometry on Swimming Performance of Helical Swimmers Using DoE

Tiantian Xu · **Gilgueng Hwang** · **Nicolas Andreff** · **Stéphane Régnier**

Abstract Helical microswimmers capable of propulsion at low Reynolds numbers have been proposed for numerous applications, ranging from in vitro tasks on lab-on-a-chip to in vivo applications for minimally invasive medicine. Several magnetically actuated helical swimmers with different geometry parameters have been proposed in prior works. However, the influence of the geometrical parameters on their swimming performance has not been clearly studied. In this paper, we propose a dimensionless study on the geometrical parameters using Design of Experiments (DoE), in order to find the influential geometrical parameters on the swimming performance. We found that the most influential geometrical parameter on the swimming performance is the pitch of the helix. A helical swimmer with longer pitch shows better swimming performance. The effects of the factors obtained by the experiments are also compared to the effects estimated by the theoretical sensitivity analysis.

T. Xu
Institut des Systèmes Intelligents et Robotique, UPMC, Paris, France & Department of Mechanical and Automation Engineering, the Chinese University of Hong Kong, Hong Kong, China.
E-mail: tiantian.xu@isir.upmc.fr, b133656@mailserv.cuhk.edu.hk

G. Hwang
Laboratoire de Photonique et de Nanostructures, Marcoussis, France
E-mail: gilgueng.hwang@lpn.cnrs.fr

N. Andreff
FEMTO-ST Institute, UFC/CNRS/ENSMM/UTBM, Besançon, France
E-mail: nicolas.andreff@femto-st.fr

S. Régnier
Institut des Systèmes Intelligents et Robotique, UPMC, Paris, France
Tel.: +33-1-44272879
E-mail: stephane.regnier@isir.upmc.fr

1 Introduction

Microrobots have a great impact in many applications [1–5]. They can be used to targetedly deliver chemical and biological substances, to remove material by mechanical means, to act as simple controllable static structures or to transmit biological data from a specific hard to reach location for in vivo applications [6], as well as to transport and assemble micro-objects for in vitro applications [7–9]. The application context often implies that the microrobots have to swim in fluids. However, at the microscale, the fluid becomes extremely viscous and the Reynolds number of the microrobots dramatically decreases. Purcell described that the swimming technique of corkscrew type rotating propulsion used by E. coli bacteria is suitable for swimming at low Reynolds numbers [10,11]. E.coli bacteria consist of a rod-shaped head and a bundle of passive flagella, which are driven by a rotary motor into a helical shape to generate a corkscrew-like motion [12].

For more than ten years, researchers have developed several kinds of magnetically actuated helical swimmers with different geometrical parameters, head shapes, and magnetic positioning, inspired by such flagella propulsions. The first helical swimmer with a total length of a few millimeters was proposed by Honda et al. in 1996 [13]. A permanent magnetic cubic head is driven wirelessly by an external rotating magnetic field. The swimming performance tests were in low Reynold number conditions. They predicted that this helical type swimming machine could still be scaled down to micrometer-size [14]. Bell et al. fabricated microscale helical swimmers in 2007 by using a self-scrolling fabrication technique [15]. They have been characterized by Zhang et al. [16,17]. This helical swimmer consisted of a helical tail made by GaAs/InGaAs and a thin-square-plate soft magnetic head on one end. Its total length is approximately 50 μm with 3.5 turns and its thickness is approximately 30 nm. In 2009, Ghosh et al. proposed even smaller helical swimmers with a diameter of 200 nm and a total length of 2 μm using the glancing angle deposition method [18]. These swimmers have spherical heads. A permanent magnetic film was evaporated onto one side of the swimmers. In our group at ISIR, Hwang et al. showed helical swimmers with electro-osmosis propulsion [19–21]. The micro helical swimmers used had a cylindrical head and a helical tail. The total length is about 70 μm. The entire surface is coated by a 10 nm thick Nickel layer. Mahoney et al. showed an open-loop controlled helical swimmer with an overall length of 5 mm with 3.5 turns using permanent magnetic head at low Reynolds numbers [22]. More recently, Tottori et al. presented a helical swimmer with a "claw" shaped holder attached to a polymer helical tail ranging from 4 μm to 64.5 μm [23]. This holder is used to transport micro objects. The specifications of the helical swimmers presented above with different geometrical parameters, head shapes and magnetic positioning are summarized in Table 1. Those geometrical parameters, head shapes and magnetic positioning were determined without optimization in terms of swimming performance. The influence of the head shapes and magnetic positioning has been studied in [24,25]. However, the influence of the tail geometrical parameters on the swimming performance has not been demonstrated.

In this paper, we focus our research on the influence of the helical swimmers tail's geometrical parameters on their swimming performance at low Reynolds num-

Table 1: Specifications of the helical swimmers presented in the state of the art.

	a	b	c	d	e	f	g
Author	Honda	Ishiyama	Zhang	Hwang	Ghosh	Mahoney	Tottori
Year	1996	2000	2007	2009	2009	2011	2012
Head shape	cube	cylinder	square-plate	cylindrical tube	sphere	cylindrical	claw
Magnetic material	SmCo5	NdFeB	Ni	Ni	NdFeB	NdFeB	Ni
Length	21.7 mm	4 mm	38 µm	62 µm	2 µm	5 mm	$4-64.5$ µm
Diameter	1 mm	2 mm	2.8 µm	2.1 µm	0.2 µm	1 mm	$1-8$ µm
Thickness	–	–	27 nm	27 nm	2 nm	0.16 mm	290 nm
Functional part	magnetic head	magnetic head	magnetic head	whole body	magnetic coating	magnetic head	magnetic coating

bers, to find the most influential geometrical parameter and to improve the shape of helical tails. In this manner, the helical tail geometrical parameters can be determined before the fabrication, and not the reverse. In order to compare the swimming performance of helical swimmers in different sizes, a dimensionless study is chosen [25]. The helical swimmers are at the millimeter scale. At this fabricated scale, the fabrication of helical swimmers is easy and low cost. However, the helical swimmers are tested in low Reynolds number liquid environments by using glycerol, known for its high viscosity. Other geometrical parameters, such as the pitch, the number of turns, the width, and the thickness, vary with respect to the Design of Experiments (DoE) method. Section 2 introduces the locomotion of helical swimmers, with a preliminary sensitivity analysis on the effect of the geometrical parameters on the swimming performance. Section 3 presents the DoE method with the choice of geometrical parameters, and the fabricated helical swimmers. Section 4 describes the experimental setup. The effects of the factors are presented in Section 5. They are also compared to the effects estimated by the sensitivity analysis. Section 6 concludes the paper and discusses about the future perspectives.

2 Locomotion of helical swimmers

2.1 Resistive Force Theory

Gray and Hancock [26] developed in 1955 a simplified Resistive Force Theory (RFT) to derive an expression for the propulsive velocity of sea-urchin spermatozoa. RFT is an intuitive approach for modelling slender body dynamics at low Reynolds numbers, which is used to determine the forces caused by velocity on an infinitesimally small length of helix by Lighthill [27]. The underlying assumption of RFT is that the hydrodynamic forces are proportional to the local body velocity, with the constant of proportionality being defined as the coefficient of resistance. The velocity v of an infinitesimally small length of the helix is decomposed into components parallel and perpendicular to the segment. The related drag forces acting on the segment in

parallel and perpendicular directions can be expressed as:

$$\mathrm{d}f_\perp = \varepsilon_\perp v_\perp \mathrm{d}s \tag{1}$$
$$\mathrm{d}f_\| = \varepsilon_\| v_\| \mathrm{d}s \tag{2}$$

where $\varepsilon_\perp$ and $\varepsilon_\|$ are the viscous drag coefficients, which have a number of empirical approximations; d_s is the volume of the infinitesimally small length of the helix.

Each force acting on an infinitesimally small segment of helix induces a subsequent torque about the helix origin. The total fluidic forces and torques on the helical swimmer can be obtained by integrating the differential forces and torques along the whole length of the helix. For steady-state motion, the external applied forces and torques on the helical swimmer have to balance the fluidic force and torque created by its rotation.

2.2 Helical propulsion model

By integrating the RFT along the direction of the helical axis, the result is a 2×2 propulsion matrix relating the velocity and rotation speed to the external forces and torques. This relationship corresponds to the 1D helical propulsion model proposed by Purcell in [10]. Only two degrees of freedom are considered: rotation at angular speed ω around its axis and translation at velocity v along that axis (see Fig. 1). This 2×2 matrix is called the propulsion matrix of the helical propeller.
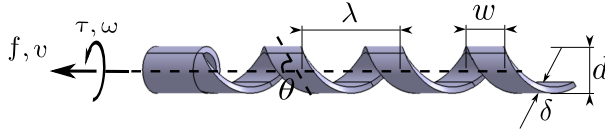

Fig. 1: 2-dof propulsion of a helical swimmer: rotation around its axis and translation along that axis [2].

Purcell proved in his paper [11] that the propulsion matrix of a helix must be symmetrical. The motion is then actually described by only three constants, that can be expressed as:

$$\begin{bmatrix} f \\ \tau \end{bmatrix} = \begin{bmatrix} a & b \\ b & c \end{bmatrix} \begin{bmatrix} v \\ \omega \end{bmatrix} \tag{3}$$

The constants a, b, c depend on the fluid viscosity η and otherwise on the geometrical parameters of the helical propeller, which include $d = 2\sigma$ defined as the diameter of the swimmer, λ defined as the pitch, θ defined as the pitch angle, w defined as the width of the tail, and δ defined as the thickness of the tail, as shown in Fig. 1. These

propulsion parameters can be computed as [2]:

$$a = 2\pi n\sigma \left(\frac{\varepsilon_\parallel \cos^2\theta + \varepsilon_\perp \sin^2\theta}{\sin\theta} \right) \tag{4}$$

$$b = 2\pi n\sigma^2 (\varepsilon_\parallel - \varepsilon_\perp) \cos\theta \tag{5}$$

$$c = 2\pi n\sigma^3 \left(\frac{\varepsilon_\perp \cos^2\theta + \varepsilon_\parallel \sin^2\theta}{\sin\theta} \right) \tag{6}$$

where n is the number of the turns of the helix, σ is the radius of the helix, and the constant $\varepsilon_\parallel$ and $\varepsilon_\perp$ are the viscous drag coefficients. According to Gray and Hancock [26], the coefficients can be expressed as:

$$\varepsilon_\parallel = \frac{2\pi\eta}{\ln(2\lambda/r) - \frac{1}{2}} \tag{7}$$

$$\varepsilon_\perp = \frac{4\pi\eta}{\ln(2\lambda/r) + \frac{1}{2}} \tag{8}$$

where η is the constant dynamic viscosity, r is the radius of the tail while the tail is circular. If the tail is not circular, the equivalent radius r can be expressed as

$$r = \frac{1}{2}\sqrt{w^2 + \delta^2} \tag{9}$$

However, the propulsion matrix in Equation (3) is validated only for a helical flagellum without a head [28]. Consider with a rigidly attached head, the propulsion matrix is modified to [2]:

$$\begin{bmatrix} f \\ \tau \end{bmatrix} = \begin{bmatrix} a + \Pi_v & b \\ b & c + \Pi_\omega \end{bmatrix} \begin{bmatrix} v \\ \omega \end{bmatrix} \tag{10}$$

where Π_v and Π_ω are respectively the translational and rotational drag coefficients for the head. The coefficients are identical for the swimmers with the same heads in the following experiments.

Helical swimmers in the following experiments are rotated by pure magnetic torques without magnetic forces, because of the uniformity of the magnetic field. Therefore, from Equation (3), the relationship between the translation velocity and rotation speed can be expressed as:

$$v = -\frac{b}{a + \Pi_v}\omega \tag{11}$$

The translational drag coefficient of the head can be expressed as $\Pi_v = 3\pi\eta d$ [29]. Therefore, the propulsion efficiency can be indicated by a coefficient E_p, which can be expressed as:

$$E_p = -\frac{b}{a + 3\pi\eta d} \tag{12}$$

The swimming performance is thus related to the geometrical parameters (pitch, width, thickness, number of turns). A sensitivity analysis of the geometrical parameters will be studied in the next section.

2.3 Sensitivity analysis

For a preliminary study of swimming performance influenced by the geometrical parameters, the simplest approach of sensitivity analysis, which is changing one-factor-at-a-time (OFAT), will be used. As a dimensionless study at low Reynolds numbers is proposed, what we are interested in is only the shape of helical tails, not the size. Therefore, the diameter of helical tails is then chosen to be fixed, because equally maximal magnetic torques are applied to each type of swimmers. So, the diameters are fixed in order to have the same magnetic head, thus to have the same magnetic torque at the same rotation frequency. Then, the influence geometrical parameters are the pitch, the number of turns, the width, and the thickness. By putting Equations (7), (8), and (9) into Equations (5) and (6), then putting Equations (5), (6), and (**??**) into (11), the propulsion efficiency as a function of, respectively, the pitch, the width, the thickness, and the number of turns can be plotted, as shown in Fig. 2, with other parameters fixed. These variation range of the geometrical parameters are chosen by the parameters of the helical swimmers in the state of the art by scaling the diameter to 1.5 mm.

From the sensitivity analysis, the pitch and the number of turns show a positive effect, and the width and the thickness show a negative effect on the swimming performance. The propulsion efficiency increases with the pitch and the number of turns, while decreases with the width and the thickness. The pitch shows the most important influence. The influences of the number of turns, the width, and the thickness are almost linear. The influence of the pitch is not linear, but monotone. For the aim of this paper, which is to find the most influential geometrical parameter, not to explore a response surface depending on the geometrical parameters, a simple linear model is adequate. The choice of models will be discussed in the next section. In order to study experimentally the influence of the geometrical parameters, including the interactions between them, a design of experiments method will be used for investigating multiple factors simultaneously, which is presented in the next section.

3 Design of Experiments

3.1 Notions

A Design of Experiments (DoE) is a series of test runs in which purposeful changes are made to the input variables of a system of process and the effects on the response variables are measured [30]. In factorial designs, multiple factors are investigated simultaneously during the test. DoE enables the reduction of the overall number of experiments, as well as to explore the interactions between factors [31]. A "factor" is defined as a controllable experimental variable, which influences the response variable [32]. The "response" is the outcome of an experiment. Each factor must assume some discrete values, defined as "levels". The changes that occur on the mean of the values of the response variable correspond to the "effects". The effects caused by the interaction of the factors can be determined as well. These interactions correspond to
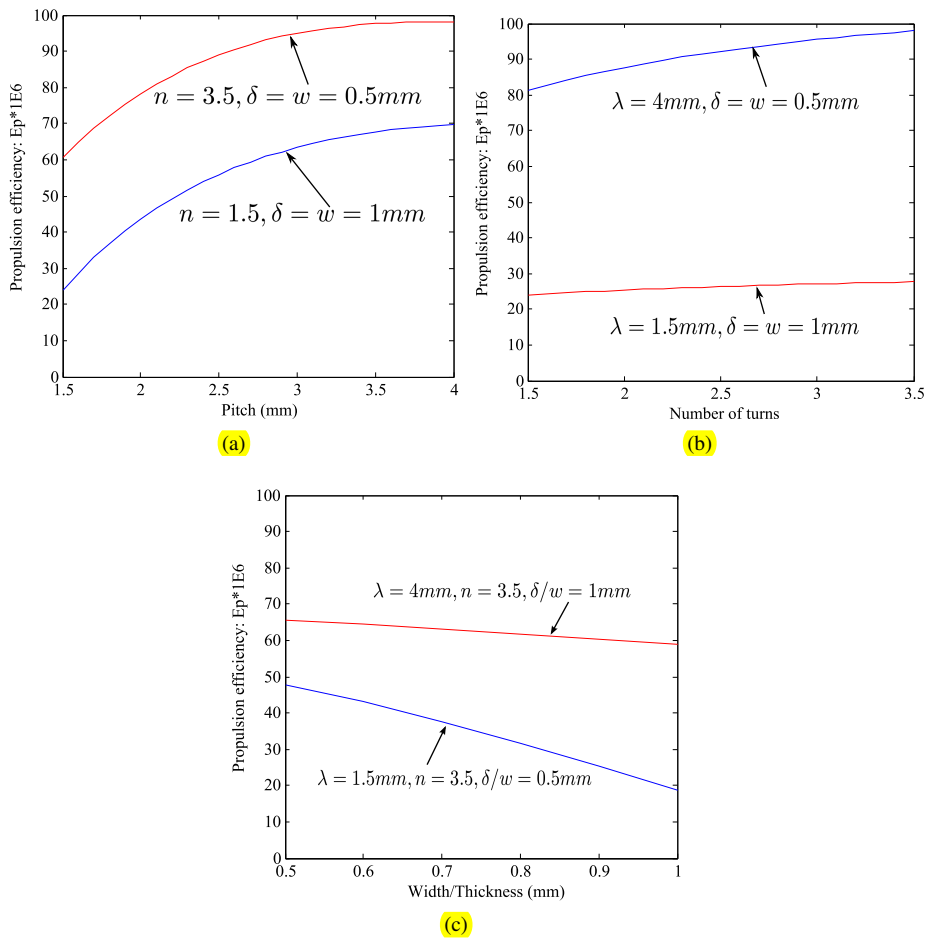
Fig. 2: Analytical estimation: (a) Propulsion efficiency as a function of pitch. (b) Propulsion efficiency as a function of number of turns. (c) Propulsion efficiency as a function of width or thickness.

combined effects, where the effect of each factor depends on the levels of the other factors.

3.2 The choice of experimental design

The objective of our experiments is to identify the geometrical parameters of helical tails that have significant effects on its swimming performance. This leads to an improvement of the geometry design.

First, a quantitative value which describes the swimming performance of a helical swimmer should be chosen as the response of the system. This response is defined

as the propulsion velocity of the helical swimmer along its axis at the same rotation frequency, which is proportional to the propulsion efficiency E_p.

Second, the factors should be determined. As presented in the sensitivity analysis (Section 2.3), the geometrical parameters that influence the swimming performance in a dimensionless condition. The four input factors are thus identified as: the pitch, the number of turns, the width, and the thickness, denoted by factors A, B, C, and D respectively. The diameter of helical tails is fixed at 1.5 mm.
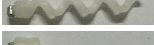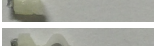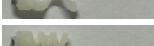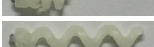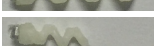
As shown in the sensitivity analysis, the influence of the geometrical parameters are all monotone, therefore, for a study of influential factor, a 2-level design is enough. A 2-level full factorial design of 4 factor requires $2^4 = 16$ different parameters design configurations. In order to decrease the cost of the experiments, a 2-level fractional factorial design of resolution III, a $2^{4-1} = 8$ fractional factorial design with 8 tests will be used [33]. The combinations of this design is depicted in Table 2. Note that the 2^{4-1} fractional factorial design estimate main effects, but these may be confounded with two-factor interactions. For example, the effect of the interaction $B \times C$ is confounded with the effect of the factor A estimated in our design. The high level $(+)$ and the low level $(-)$ are defined for each factor referencing the parameters of helical swimmers in the state of the art by scaling the diameter to 1.5 mm. A supplementary test with zero-level will be made to validate the monotony of the geometrical parameter influence.

Table 2: The fractional factorial design for 4 factors and 2 levels, with a central point for validation. The designed high level and the low level are shown.

Swimmer Index	Factors				Interactions						Response
	A	B	C	D	AxB	AxC	AxD	BxC	BxD	CxD	
	Pitch	Nb	Width	Thickness							
$-$	1.5 mm	1.5	0.5 mm	0.5 mm							
$+$	4 mm	3.5	1 mm	1 mm							
0	2.75 mm	2.5	0.75 mm	0.75 mm							
1	$-$	$-$	$+$	$-$	$+$	$-$	$+$	$-$	$+$	$-$	R_1
2	$+$	$-$	$-$	$-$	$-$	$-$	$-$	$+$	$+$	$+$	R_2
3	$-$	$+$	$-$	$-$	$-$	$+$	$+$	$-$	$-$	$+$	R_3
4	$+$	$+$	$+$	$-$	$+$	$+$	$-$	$+$	$-$	$-$	R_4
5	$-$	$-$	$+$	$+$	$+$	$-$	$-$	$-$	$-$	$+$	R_5
6	$+$	$-$	$-$	$+$	$-$	$-$	$+$	$+$	$-$	$-$	R_6
7	$-$	$+$	$-$	$+$	$-$	$+$	$-$	$-$	$+$	$-$	R_7
8	$+$	$+$	$+$	$+$	$+$	$+$	$+$	$+$	$+$	$+$	R_8
9	0	0	0	0	0	0	0	0	0	0	R_9

This table of test matrix will guide us in designing the geometrical parameters of the helical swimmers. The specification of the eight designed helical swimmers with different geometrical parameters are described in Table 3. Their swimming performance will be compared in Section 5.

Table 3: Specifications of the helical swimmers for full factorial design with DoE of 4 factors and 2 levels with a central point for validation.

	Diameter (mm)	Pitch (mm)	Nb	Width (mm)	Thickness (mm)	Image
1	1.5	1.5	1.5	1	0.5	
2	1.5	4	1.5	0.5	0.5	
3	1.5	1.5	3.5	0.5	0.5	
4	1.5	4	3.5	1	0.5	
5	1.5	1.5	1.5	1	1	
6	1.5	4	1.5	0.5	1	
7	1.5	1.5	3.5	0.5	1	
8	1.5	4	3.5	1	1	
9	1.5	2.75	2.5	0.75	0.75	

4 System overview

4.1 Helical swimmers at low Reynolds numbers

The helical swimmers with diameters of 1.5 mm are made of plastic Accura 25 by rapid prototyping with the geometrical parameters presented in Table 3. An example of helical swimmer 4 is depicted in Fig. 3. Each one has a cylindrical head with a slit in the middle. A cylindrical permanent magnet magnetized in the axis with 1 mm of diameter and 1.5 mm of length is seated in the slit. As the magnetization direction is perpendicular to the axis of the helical swimmer, the swimmer is thus driven by a rotating magnetic field around its propelled axis.
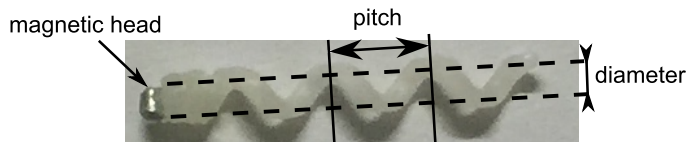

Fig. 3: Picture of helical swimmer 4.

A helical swimmer with a magnetic head shows a step-out frequency: below the step-out frequency, it rotates in sync with the external rotating magnetic field; beyond this step-out frequency, its rotation frequency decreases [25]. Therefore, below the step-out frequency, the magnitude of the magnetic field has no influence on the swimming performance of helical swimmers. The step-out frequency depends on the Reynolds number. In the following experiments, the helical swimmers are in pure

glycerol liquid. The glycerol density measured by a portable densitometer (DMA 35) is $1.26 \times 10^3 \text{ kg/m}^3$. The viscosity of glycerol measured by a falling ball viscometer (Brookfield KF10) is 1350 mPa·s at 23 °C. The helical swimmers swim at 0.1 mm/s − 1.5 mm/s in the experiments. The calculated Reynolds numbers in the following experiments are $Re \approx 10^{-4} - 1.5 \times 10^{-3}$. Meanwhile, in water, a swimming bacterium such as E.coli has a $Re \approx 10^{-5} - 10^{-4}$ [34], the artificial bacteria flagella swim at $Re \approx 10^{-4}$ [16]. The step-out frequency of the used helical swimmers in pure glycerol was measured as 5 Hz with a magnetic field of 10 mT. The rotation frequency of the magnetic field is always below the step-out frequency in the following experiments, so that the helical swimmers is supposed to rotate synchronously with the magnetic field.

4.2 Magnetic actuation system

Three orthogonally arranged Helmholtz coil pairs are used to generate a rotating magnetic field, as shown in Fig. 4a. Each set of Helmholtz coils is driven by an ADS 50/5 4-Q-DC servoamplifier of Maxon Motor Control, capable of 5 A continuous current and 10 A peak current. The amplifiers are powered by a TDK-Lambda SWS300-48 DC power supply, capable of 6.7 A current. The output voltage of the power supply is 48 V. The amplifiers are used on current control mode. Analog communication between the PC and the amplifiers is accomplished with a Sensoray 626 Analog and Digital I/O card. The magnetic fields generated by the three coil pairs were measured and calibrated by a gaussmeter Hirst GM08. The magnetic flux density used in the experiments is 10 mT. The magnetic field rotates at 3 Hz. The helical swimmers are in a beaker filled with glycerol, which are put in the center of the Helmholtz coils. Fig. 4b shows a view from the top.
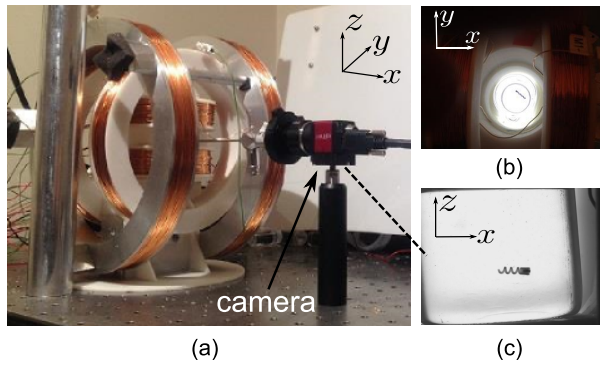

Fig. 4: (a) Helmholtz coils setup with a camera. (b) The helical swimmer viewed from the top. (c) Image taken by the camera.

4.3 Swimming performance estimation

The swimming performance is defined as the propulsion velocity of the helical swimmer during the propulsion as mentioned in Section 3.2. The propulsion experiments were recorded by a firewire camera (Guppy Pro F032) with a framerate of 25 Hz. A LED is placed behind to light the scene. Fig. 4c shows an image taken by the camera.

During the propulsion, the helical swimmer sank down because of its own gravity. However, this sinking velocity is not relevant to the swimming performance. Only the propulsive velocity v_x of the helical swimmer generated by the rotating magnetic field in the horizontal plane xOy is interested. It is calculated by the travelled pixels per second, and then converted to millimeters per second with the calibration information of the camera.

5 Experimental results

5.1 Swimming performance estimation

The helical swimmers are actuated by a rotating magnetic field of 10 mT and 3 Hz. The axis of the rotating field is in the horizontal plane. Only the propulsion velocity in the horizontal plane is useful to compare the swimming performance. For each of the nine helical swimmers, three tests are realized. The average velocity of the three tests is used for the effect estimation. The swimming performance of helical swimmers with incertitudes are expressed in Fig. 5. The effect of the geometrical parameters' influence will be estimated in the next section.
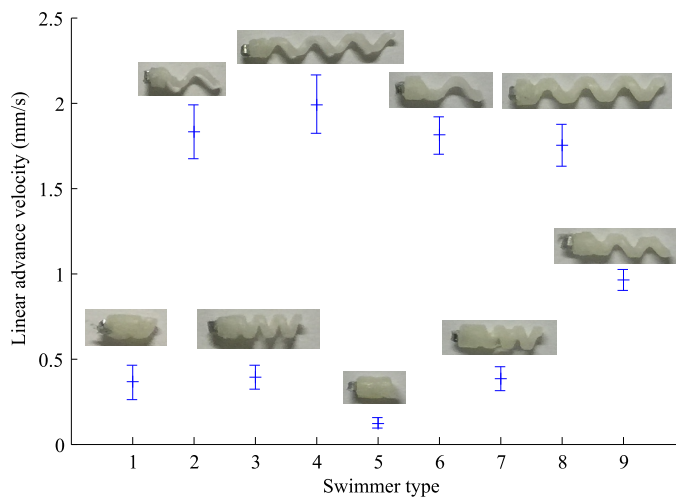

Fig. 5: Swimming velocities in the horizontal plane for different helical swimmers in glycerol within 10 mT magnetic field and 3 Hz of rotation frequency.

5.2 Impact of the geometrical parameters

The effect of the factors and the possible interactions are evaluated by the difference of the average response values for each factor or interaction at its high level ($+$) and that at its low level ($-$). For example, the effect for the pitch (factor A), noted as Y_A, can be expressed as:

$$Y_A = \frac{R_2 + R_4 + R_6 + R_8}{4} - \frac{R_1 + R_3 + R_5 + R_7}{4} \tag{13}$$

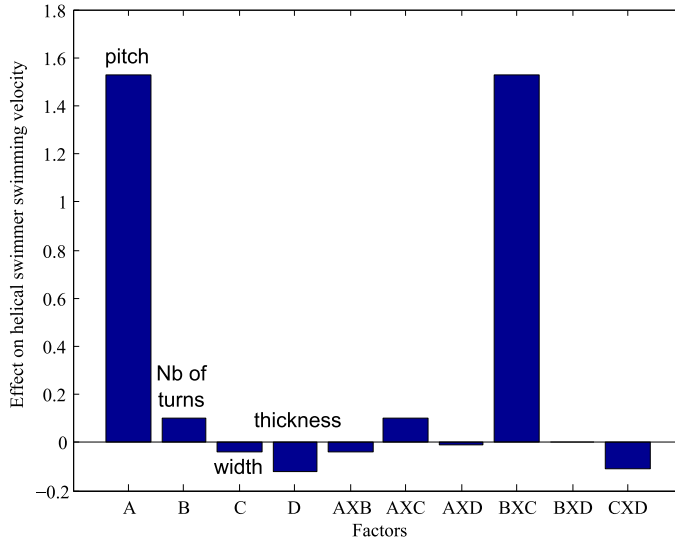The validation swimmer (swimmer 9) with zero level proves the monotony of the effects of the factors.

Fig. 6: The effect of factors and interactions on swimming velocity estimated with a 2^{4-1} fractional factorial design.

These effects of the factors and their interactions are depicted in Fig. 6. The pitch shows a significant positive effect since Y_A is positive and high. The number of turns shows a non-important positive effect compare to the effect of the pitch. Both the width and the thickness show non-significant negative effects, because Y_C and Y_D are negative. The effects of the main factors estimated by the experiments with geometrical parameters of a 2^{4-1} fractional factorial design are coincident with those of the sensitivity analysis of OFAT estimated in Section 2.3. The pitch is thus the most influential geometrical parameter on the swimming performance of helical swimmers at low Reynolds numbers. The helical swimmers with longer pitch swim significantly faster than those with shorter pitch in the same rotating magnetic field. The helical swimmers with smaller width and thickness swim slightly faster. Note that the obtained optimized ratio of the pitch and the diameter (4 mm for the pitch, and 1.5 mm

for the diameter) is similar than that of the E. coli bacteria, which are ranging from $2-4\ \mu m$ for the pitch and $0.7-1.4\ \mu m$ for the diameter [35]. For a physical insight, the width and the thickness have a negative effect, because swimmers with smaller width and thickness have lower fluidic drags, thus a higher swimming performance. Both the pitch and the number of turns have positive effects, because the propulsive force is integrated along the total length of the swimmer, which increases with the pitch and the number of turns. However, by increasing the number of turns, the fluidic drags are also much increased. Therefore, the effect of the pitch is more significant than that of the number of turns. However, we should note that although the helical swimmers with tails of smaller widths show better swimming performance, their mechanical structures are more fragile. In order to have a compromise between the swimming performance and the solidness of helical swimmers, a minimum of width should be imposed.

As mentioned in Section 3.2, for the chosen fractional factorial design of resolution III, presented in Table 2, the effect of the interaction $B \times C$ is confounded with the effect of the main factor A. Therefore, the effect of the interaction $B \times C$ can not be estimated independently. In order to estimate the effect of the interaction $B \times C$, we eliminate the factor D, which shows non-significant effect including the interactions, and redesign a $2^3 = 8$ full factorial design with 3 factors A, B, and C. Note that, 4 combinations of the geometrical parameters in this 2^3 design have already been made in 2^{4-1} fractional factorial design. Only four more combinations have to be tested. In total, we have tested 12 combinations of geometrical parameters, which is more efficient than a 2^4 full factorial design with 4 factors including 16 combinations of geometrical parameters. The effects of the factors A, B, C, and their interactions are shown in Fig. 7. At this time, the effect of the interaction $B \times C$ is estimated independently, and presents a non-significant effect. As a conclusion, no two-factor interaction shows a significant effect. Even high-order interactions are thus negligible.

6 Conclusions

In this paper, we compared the swimming performance of helical swimmers with different geometrical parameters, including the pitch, the number of turns, the width, and the thickness. First, the experiments are defined by a 2^{4-1} fractional factorial design with 2 levels and 4 factors, in order to estimate the influential geometrical parameters and interactions. The study is dimensionless with a fixed diameter of the helical swimmers. The swimmers are in millimeter scale and at low Reynolds numbers. According to the estimation of the effect of 4 different factors, the pitch is the most influential factor for swimming performance of a helical swimmer. The influence of the pitch is positive, which means that helical swimmers with longer pitches show better swimming performance. The influence of the number of turns, the width and the thickness are less significant. The number of turns has a positive effect. The width and the thickness have both negative effects. The effects of the factors are coincident with theoretical sensitivity analysis. As the effect of interactions can not be estimated independently in a fractional design, a full factorial 2^3 design with 3 factors
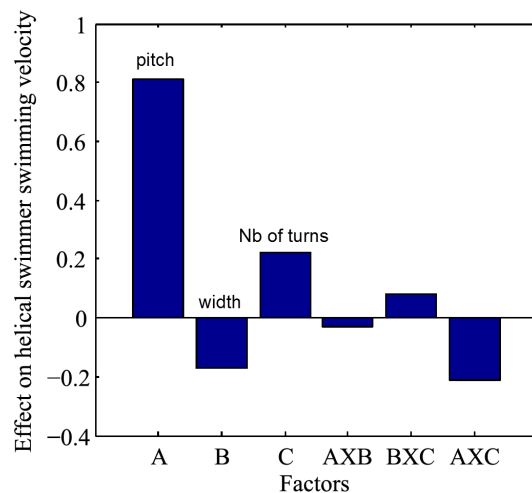
Fig. 7: The effect of factors and interactions on swimming velocity estimated with a 2^3 full factorial design.

are completed to show that no two-factor interaction shows a significant effect. An improved geometry design of helical swimmers can be thus proposed by increasing its pitch.

References

1. J. Abbott, Z. Nagy, F. Beyeler, B. Nelson, Robotics Automation Magazine, IEEE **14**(2), 92 (2007). DOI 10.1109/MRA.2007.380641
2. J. Abbott, M. Cosentino Lagomarsino, L. Zhang, L. Dong, B. Nelson, The International Journal of Robotics Research **28**(11-12), 1434 (2009)
3. M. Gauthier, S. Régnier, *Robotic Micro-assembly* (IEEE press, 2010)
4. N. Chaillet, S. Régnier, *Microrobotics for Micromanipulation*. ISTE (Wiley, 2013)
5. M. Sitti, H. Ceylan, W. Hu, J. Giltinan, M. Turan, S. Yim, E. Diller, Proceedings of the IEEE **103**(2), 205 (2015)
6. B. Nelson, I. Kaliakatsos, J. Abbott, Annual Review of Biomedical Engineering **12**(1), 55 (2010)
7. A. Bolopion, H. Xie, S. Haliyo, S. Régnier, IEEE/ASME Transaction on Mechatronics **17**(1), 116 (2012)
8. M. Hagiwara, T. Kawahara, T. Iijima, F. Arai, Robotics, IEEE Transactions on **29**(2), 363 (2013). DOI 10.1109/TRO.2012.2228310
9. M. Gauthier, N. Andreff, E. Dombre, *Intracoporeal robotics: from milliscale towards nanoscale* (Wiley, 2014). ISBN:978-1-84821-371-5
10. E. Purcell, American Journal of Physics **45**(1), 3 (1977)
11. E. Purcell, Proc. Natl. Acad. Sci. U.S.A. **94**(21), 11307 (1997)
12. H. Berg, R. Anderson, Nature **245**(5425), 380 (1973)
13. T. Honda, K. Arai, K. Ishiyama, Magnetics, IEEE Transactions on **32**(5), 5085 (1996)

14. K. Ishiyama, K. Arai, M. Sendoh, A. Yamazaki, in *Micromechatronics and Human Science, Proceedings of 2000 International Symposium on* (2000), pp. 65 –69
15. D. Bell, S. Leutenegger, K. Hammar, L. Dong, B. Nelson, in *Robotics and Automation, 2007 IEEE International Conference on* (2007), pp. 1128 –1133
16. L. Zhang, J. Abbott, L. Dong, K. Peyer, B. Kratochvil, H. Zhang, C. Bergeles, B.J. Nelson, Nano Letters **9**, 3663 (2009). DOI 10.1021/nl901869j
17. L. Zhang, K. Peyer, B. Nelson, Lab Chip **10**, 2203 (2010)
18. A. Ghosh, P. Fischer, Nano Letters **9**(6), 2243 (2009)
19. G. Hwang, S. Haliyo, S. Régnier, in *Robotics Science and Systems* (2010)
20. G. Hwang, R. Braive, L. Couraud, A. Cavanna, O. Abdelkarim, I. Robert-Philip, A. Beveratos, I. Sagnes, S. Haliyo, S. Régnier, The International Journal of Robotics Research **30**(7), 806 (2011)
21. J. Acosta, G. Hwang, J. Polesel-Maris, S. Régnier, Review of Scientific Instruments **82**(3), 035116 (2011)
22. A. Mahoney, J. Sarrazin, E. Bamberg, J. Abbott, Advanced Robotics **25**(8), 1007 (2011)
23. S. Tottori, L. Zhang, F. Qiu, K. Krawczyk, A. Franco-Obregn, B. Nelson, Advanced Materials **24**(6), pp. 811 (2012). Highlighted as the front cover
24. T. Xu, G. Hwang, N. Andreff, S. Régnier, in *Advanced Intelligent Mechatronics (AIM), 2013 IEEE/ASME International Conference on* (IEEE, 2013), pp. 1114–1120
25. T. Xu, G. Hwang, N. Andreff, S. Régnier, Mechatronics, IEEE/ASME Transactions on **19**(3), 1069 (2014)
26. J. Gray, G.J. Hancock, J. Exp. Biol. **32**(4), 802 (1955)
27. J. Lighthill, SIAM Review **18**(2), 161 (1976)
28. B. Rodenborn, C.H. Chen, H.L. Swinney, B. Liu, H. Zhang, Proceedings of the National Academy of Sciences **110**(5), E338 (2013)
29. K.B. Yesin, K. Vollmers, B.J. Nelson, International Journal of Robotics Research **25**(5-6), 527 (2006)
30. R.A. Fisher, *The Design of Experiments* (Olyver and Boyd Edinburgh, 1935)
31. J. Goupy, L. Creighton, *Introduction aux plans d'expériences - 3ème édition*. Technique et ingénierie: Série conception (Dunod, 2006)
32. R.L. Mason, R.F. Gunst, J.L. Hess, *Statistical Design and Analysis of Experiments*, 2nd edn. WILEY SERIES IN PROBABILITY AND STATISTICS (WILEY & SONS, 2003)
33. G.E.P. Box, J.S. Hunter, W.G. Hunter, Statistics for Experimenters An Introduction to Design (1976)
34. E. Lauga, T. Powers, Reports on Progress in Physics **72**(9), 096601 (2009)
35. U. Moran, R. Phillips, R. Milo, Cell **141**(7), 1262 (2010)